Journal of the European Ceramic Society 20 (2000) 707–713

Combustion-synthesis of $SrTiO_3$ Part I. Synthesis and properties of the ignition products

J. Poth, R. Haberkorn, H.P. Beck*

Department of Inorganic and Analytical Chemistry and Radiochemistry, University of Saarland, 66123 Saarbruecken, Im Stadtwald, Gebaeude 23.1, Germany

Received 30 March 1999; received in revised form 24 June 1999; accepted 3 July 1999

Abstract

Nanosized powders of $SrTiO_3$ have been prepared via combustion synthesis. Aqueous solutions of the metal nitrates and differing amounts of EDTE as reducing and NH_4NO_3 as oxidizing reactant were evaporated and the resulting solid mixtures were ignited at different temperatures. As determined form XRD, the products exhibit crystallite sizes up to 42 nm with high microstress values resulting from the short reaction time. Crystallite size distributions were mostly very broad and could not be described by a single log-normal function, these results were confirmed by TEM images. The properties of the products could be explained as depending on the composition of the educt mixtures and the ignition temperatures.

Keywords: Combustion synthesis; $SrTiO_3$; Titanates; X-ray methods

1. Introduction

Earthalkaline Titanates like $SrTiO_3$ are materials widely used in microelectronic devices. Important applications are its use as a substrate for the heteroepitaxial growth of high-T_C-superconductors[1–3] or in solid solutions with $BaTiO_3$ in chemical sensors,[4] multi-layer capacitors and DRAM devices.[5–7] The miniaturization of such devices makes it necessary to synthesize nanosized powders or thin films of these materials with high homogeneity and low impurity levels. Typical preparation routes are chemical solution deposition,[5–7] sol–gel methods,[8] the thermal decomposition of mixed citrate or oxalate complexes,[9] hydrothermal methods[10,11] or freeze drying of nitrate solutions.[12] A new preparation route uses exothermic reactions such as combustion methods or self-propagating high-temperature syntheses (SHS).[13–16] A solid mixture of oxidizing and reducing reactants is ignited thermally and a rapid, strong exothermic reaction takes place which produces a lot of gases and the desired ceramic powder as the only solid product. The oxidizing reactants are often nitrate ions introduced by the use of metal nitrates and/or the addition of NH_4NO_3 to the mixture. As reducing reactant, a lot of organic compounds can be used. Ethylene diamine tetraacetic acid (EDTA) and other polycarboxylic acids are often used because of their property to form stable watersoluble complexes with most metal cations; thus the synthesis of a homogeneuous solution of the starting materials is provided which can easily form a solid reaction mixture without demixing by evaporating or spray-drying. In this work, $SrTiO_3$ was used instead of $BaTiO_3$ as a model substance because of its cubic symmetry which simplifies the evaluation of X-ray data, the lower thermodynamic stability of its 'intrinsic' impurities like $SrCO_3$ and its lower probability to form phases with an A:B ratio differing from1 except for the Ruddlesden–Popper phases $Sr_{n+1}Ti_nO_{3n+1}$, $n=1,2,\ldots\infty$. The influence of reaction parameters like the amounts and ratios of oxidizing and reducing reactants and the ignition temperatures is studied, the second part in a forthcoming paper[18] describes the behaviour of the ignited specimens during sintering.

2. Experimental

2.1. Sample preparation

The starting materials were $Sr(NO_3)$, $TiCl_4$, EDTA and NH_4NO_3, purities above 98%, the Ba-content of

* Corresponding author Tel.: +49-0681-302-2421; fax: +49-0681-302-4233.

E-mail address: hp.beck@rz.uni-b.de (H.P. Beck).

0955-2219/00/$ - see front matter
PII: S0955-2219(99)00190-9

$Sr(NO_3)_2$ was $<0.05\%$. To yield $TiO(NO_3)_2$, $TiCl_4$ was hydrolized in chilled water and precipitated in cold 1 m NH_3. The resulting TiO_2 gel was washed with deionized water to remove residual chloride ions and then dissolved with 7 M HNO_3; the molar ratio of HNO_3 to Ti was 5. The titanium content in the resulting solution was determined gravimetrically.

To prepare the reaction mixtures, $Sr(NO_3)_2$, EDTA and NH_4NO_3 were dissolved in distilled water and neutralized with 12 M NH_4OH. Then the $TiO(NO_3)_2$ solution was added and neutralized again. Thus the molar ratio of NH_4NO_3 to Sr and Ti was 7 if no additional NH_4NO_3 was added.

The chosen compositions were: (I to V = number of the mixture)

I:Sr:Ti:EDTA	1:1:1,	7 NH_4NO_3	(i.e. no further addition of NH_4NO_3)
II:Sr:Ti:EDTA	1:1:1,	15 NH_4NO_3	
III:Sr:Ti:EDTA	1:1:2,	7 NH_4NO_3	(i.e. no further addition of NH_4NO_3)
IV:Sr:Ti:EDTA	1:1:2,	25 NH_4NO_3	
V:Sr:Ti:EDTA	1:1:2,	40 NH_4NO_3	

The solutions were evaporated on a heater plate under stirring at about 80°C until a homogenuous, white gel was obtained. These gels were then dried for some hours at 110–130°C in a drying oven. The resulting brown, brittle masses were kept dry in a desiccator until they were ignited in a corundum crucible preheated to ignition temperature in a muffle furnace. The crucible was removed from the furnace immediatly after the end of the reaction which only took a few seconds or after a heat treatment of one minute in the cases where the ignition temperature was too low to achieve a self-propagating reaction. A complete reaction under participation of only the mixture compounds should be reached for a ratio of EDTA:NH_4NO_3 of 1:15:

$$Sr(NO_3)_2 + [TiC_{10}H_{12}N_2O_8] + 15NH_4NO_3 \rightarrow SrTiO_3 + 10CO_2 + 17N_2 + 36H_2O$$

Since the reactions take place in ambient atmosphere, there is always some oxygen from air participating in the oxidation of the mixture; for each oxygen atom from the atmosphere taking part in the reaction, one NH_4NO_3 less is needed. It can also be observed that especially for mixtures with low reactivity, i.e. low NH_4NO_3 content and thus lower heat evolution, an incomplete combustion of EDTA takes place. These two facts make it difficult to describe the burning process and to determine a reaction equation; the equation above can only describe an ideal process. Results of DTA/TG—measurements in which the precursors are heated slowly can not be compared with the ignition process used here where the precursors are heated at a rate of several hundred K/s.

2.2. Determination of metrics and microstructural parameters

For the characterization of nanoscaled materials, parameters such as crystallite size, size distribution and microstress are important in addition to the metric parameters of the compound. The first two may be extracted from a statistical evaluation of TEM-images, but a sophisticated evaluation of X-ray powder diagrams will also give this information together with the other parameters mentioned. We have focussed our efforts on the development of procedures to extract such information from XRD without the need of a fourier transform as used in Warren–Averbach analysis. Our program code FormFit[17] allows the determination of metric and microstructural parameters.

Similar to the Rietveld method, an analytical function is used to describe the measured X-ray pattern. Each line of the pattern is described by a split pseudo-Voigt function with the line width B, the Lorentzian fraction n and asymmetry term z, which are all developed as a function of 2θ. The functions for B, n and z have each three parameters for describing the apparative effect which is determined empirically from a pattern of LaB_6 as standard material which shows little to no microstructural effects.

The microstructure of the specimen itself, i.e. crystallite sizes D_{Vol} and microstrain e, can then be determined separately from the diagrams taking into account the apparative intensity distribution function and the different functions which describe the angle dependency of the line width from such microstructural parameters. We then assume a log-normal distribution of diameters D of spherical crystallites with the median D_0 and a variance parameter σ. Having put up an empirical relationship between this variance and the parameter n describing the Lorentzian fraction, we can derive all parameters of such a size distribution from our X-ray powder diagrams and not only the mean column height as most other programs do. Values derived for D_V, σ and e are given in the tables.

All XRD-data were taken on a Siemens D5000-diffractometer with Cu-$K_{\alpha 1}$-radiation.

3. Results

3.1. Influence of the ratio of EDTA:NH_4NO_3

To examine the influence of the EDTA/NH_4NO_3 content, all mixtures were ignited at 600°C. One should

expect that the more reactive the mixture is, i.e. the higher the ratio of NH_4NO_3 to EDTA, the more crystalline and pure are the products obtained for the same ignition temperature.

The most reactive mixture II undergoes an almost explosion-like reaction which is finished after a few seconds, while the least reactive mixture III only smokes and even does not glow. The colours of the products vary from white for mixture II over greyish for V, dark grey for I and IV to an ash-like black for mixture III. This is caused by different amounts of residual amorphous carbon-containing compounds resulting from the more or less incomplete oxidation of EDTA.

Fig. 1 shows the XRD-patterns of the ignited powders (600°C). The results of thermogravimetry and fitting of the XRD-data are listed in Table 1. The results are:

(a) the higher the amount of oxidizing reactant compared to reducing reactant, the more crystalline is the product and the less is the amount of unburned residues;
(b) low total combustible contents lead — independent of the ratio of oxidizing to reducing reactant — to the formation of $SrCO_3$, Sr_2TiO_4, amorphous TiO_2 and some amorphous, unburned, carbon-containing phases as impurities. High contents produce only amorphous phases in different amounts of such impurities;
(c) mostly the products exhibit large lattice constants and microstress values.

3.2. Influence of ignition temperature

The influence of the ignition temperatures (in the following abbreviated as iT) depends on the composition of the mixtures:

(a) for very reactive mixtures (II/IV), the influence of the iT is small; once the mixture ignites, the heat evolution is so high that the ambient temperature is meaningless. For lower total combustible contents (in the following abbreviated as tcc), crystalline impurities like $SrCO_3$ appear, while higher tcc only produce amorphous residues resulting from an incomplete reaction. The total content of these impurities is small;
(b) mixtures of medium reactivity with lower total combustible contents (I): at low iT, a lot of undesired crystalline phases and unburned residues can be observed. At higher iT, $SrTiO_3$ is the only crystalline phase;
(c) mixtures with medium or low reactivity and higher tcc: low iT lead to amorphous products. With increasing iT, the crystallinity of the product increases, and except for small amounts of almost amorphous $SrCO_3$ which are sometimes formed, the desired product is the only crystalline phase generated.

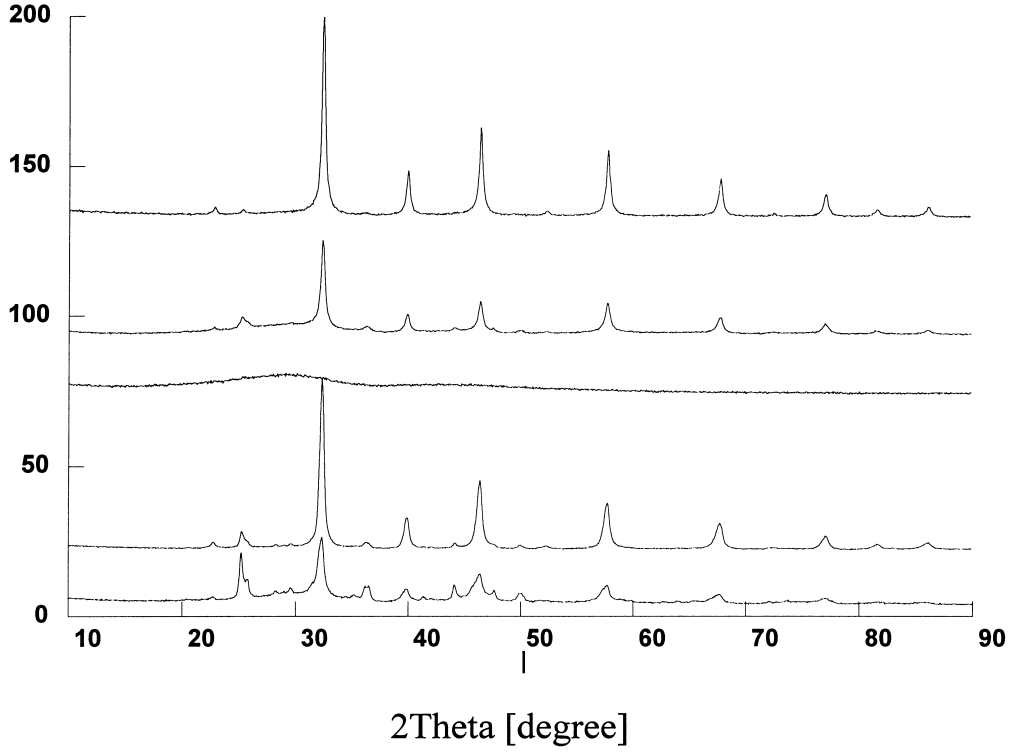

Fig. 1. From bottom to top: mixt. I to V, ignited at 600°C.

Table 1
Characteristics of differently prepared materials[a]

Mixt/iT	Δm (%)	a (pm)	D_v (nm)	e (%)	σ	Group
I/400°C	21	–	–	–	–	I
I/600°C	16	–	–	–	–	I
I/800°C	8	391.05(1)	24	0.336(9)	1.73	I
I/900°C	4	390.59(2)	14	0.04(1)	>>2	IV
I/1000°C	<2	390.63(1)	36	0.13(1)	>>2	IV
II/400°C	2	391.99(2)	26	0.43(1)	1.65	II
II/600°C	<2	391.29(2)	30	0.36(1)	1.66	II
III/600°C	44	Amorphous				III
III/900°C	8	390.54(1)	31	0.11(1)	1.86	(IV)
IV/400°C	33	Amorphous				III
IV/600°C	22	390.63(3)	28	0.28(4)	>2	III
IV/800°C	4	390.70(2)	18	0.36(1)	>>2	IV
IV/900°C	<2	390.66(1)	42	0.17(1)	1.53	IV
V/400°C	14	390.54(1)	26	0.22(1)	>>2	IV
V/600°C	6	390.54(1)	31	0.19(1)	>>2	IV
V/800°C	<2	390.60(1)	20	0.23(1)	>>2	IV

[a] Δm, thermogravimetric weight loss of the product under ambient atmosphere up to 1200°C; a, lattice constant; single crystal 390.55 pm; D_v, medium volume weighted crystallite size; e, medium microstresses; σ, width of the crystallite size distribution for an assumed log-normal distribution (annotations in Discussion); –, high uncertainty of the refined values, no useful results; values in brackets are the estimated standard deviation for the last number.

XRD-patterns of mixtures I and IV which are used as examples are shown in Figs. 2 and 3, the results of refinement are given in Table 1.

4. Discussion

First of all, one has to consider the various reaction parameters which are

- ignition temperature
- temperature reached during reaction and heat evolution
- gas evolution

and the reaction time during which heat and gas are generated.

The iT is given by the furnace and crucible. The reaction temperature can be measured by a flame pyrometer as some authors report and reaches more than 1000°C for mixtures whose reactivity can be compared to the very reactive ones in this work;[13–15] the temperature could not be measured by our means. By exact repetition of the procedure, the results are surprisingly reproducible. The materials show similar to equal characteristics, especially in view of such parameters as size, size distribution and microstress. Almost all thermal energy produced during reaction is dissipated by the gases evolved. This means there is neither mass nor energy conservation. This and the fact that the burning process almost always produces amounts of other phases — both solid and gaseous — than those given in the ideal reaction equation above make a quantitative thermodynamic treatment of the burning process very difficult. The gas evolution depends on the total combustible contents and their kind and degree of conversion to gaseous phases during reaction. The reaction time decreases with increasing reactivity of the mixtures and with increasing iT. Short reaction times mean high gas evolution rates.

The influence of all these parameters can be given in short as follows:

- At higher iT, the educts decompose faster, the reaction accelerates and the heat production rises. This increases the reaction temperature, and if it is increased strongly enough, the reaction becomes self-propagating.
- A higher reaction temperature causes a more complete reaction and enhances sintering of the products.
- A higher gas evolution will hinder the sintering of the products.

The combination of these factors explains the characteristics of the products obtained:

(a) At lower iT, mixtures with lower tcc show crystalline impurities like $SrCO_3$ and Sr_2TiO_4, mixtures with higher tcc do not: the higher the dilution of the metal cations in the combustible matrix and the higher the gas evolution during the reaction, the lower is the probability of formation of crystalline impurities which may be detected in XRD.

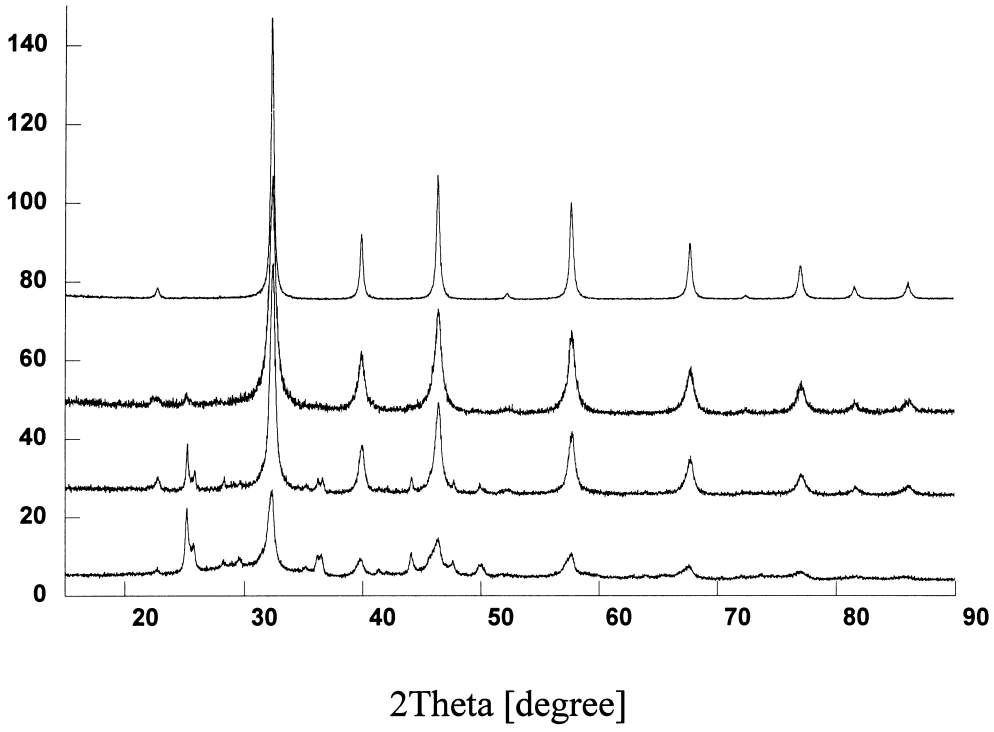

Fig. 2. From bottom to top: mixt. I, ignited at 600, 800, 900, 1000°C.

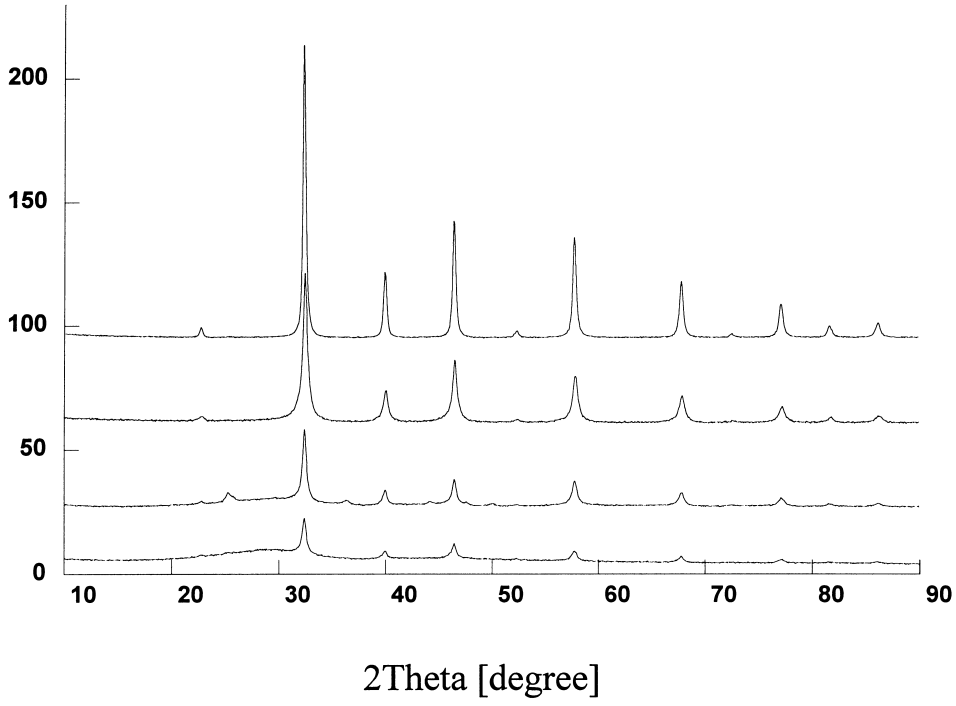

Fig. 3. From bottom to top: mixt. IV, ignited at 400, 600, 800, 900°C.

(b) Higher reactivity lowers the influence of the iT: at low iT the reaction enthalpy is already so high that the reaction produces more energy than can be dissipated by the gases produced once the reaction has started.

(c) The large lattice constants and microstress values (see Table 1) are a consequence of the short reaction times, the lattice cannot arrange itself completely especially at the surface of the crystallites and unburned impurities may expand it additionally.

(d) For mixtures with medium and lower reactivities: as soon as $SrTiO_3$ is formed, its crystallite size stays more or less the same for increasing iT and then abruptly grows (e.g. I: 900/1000°C; IV: 800/900°C): At low iT, some crystallite seeds of the size of only a few elementary cells are formed. These seeds can grow by agglomeration — only in this early state — and adsorption of amorphous material around them, but only to a size between 20 and 30 nm. With higher iT, more seeds are generated and the amount of thermodynamically less stable phases — amorphous or crystalline — decreases, but the reaction temperature is still not high enough for the seeds to grow. A further increase in iT pushes the reaction temperature over the threshold for seed growth, the crystallite size increases.

(e) The crystallite size distributions (see Table 1) are always very broad except for a few cases. Some of the crystallite seeds grow to the above mentioned size of 20–30 nm, but when the reaction is over there are still a lot of smaller crystallites. The exceptions where the size distributions are more narrow have one thing in common: a high reaction temperature in addition to a not too high gas evolution rate. The surface energy of the small crystallites is so high at these temperatures that they sinter together almost immediately if they contact. But if the gas evolution rate further increases, it becomes predominant and hinders sintering again, the width of the size distribution is high: see mixture V, all iT.

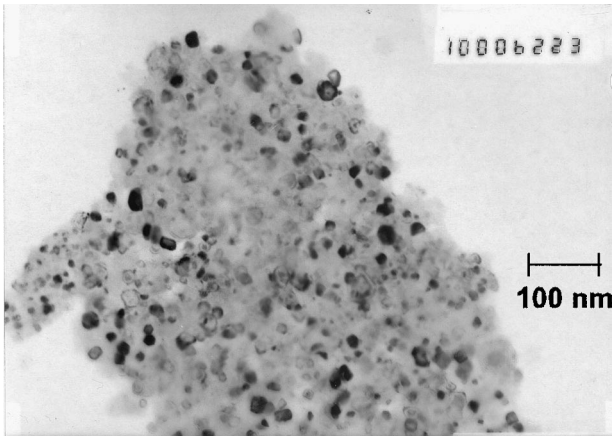

Fig. 4. TEM-image of mixt. IV, ignited at 800°C.

The validity of such statements about seed growth and crystallite size distributions can be proven by TEM images. Fig. 4 shows a TEM-image of mixture IV, ignited at 800°C and left in the oven for 1 min, other images of the same specimen show the same characteristics. A histogram for 699 crystallites is given in Fig. 5. Details smaller than 5 nm are difficult to inspect because of the resolution of the microscope available, but there seems to be a large number of particles which are still smaller. This leads to the assumption that the burning process generates a lot of crystallites of 5 nm and smaller which immediately begin to grow, but this process is stopped before completion by the short reaction time. A log-normal distribution would be reached when the smaller crystallites have disappeared, but the distribution in the products is rather a sum of at least two log-normals, e.g. one for the original and one for the grown crystallites. It is nevertheless possible to use our mathematical method to derive a mean σ which will approximately describe the situation by a single log-normal distribution.

This was confirmed by a simple experiment: amounts of the same mixture were ignited again at 800°C and left in the oven for 2 resp. 3 min and 2 h. The only X-ray diffracting phase was always $SrTiO_3$. The values of the Lorentzian fraction n giving information about the distribution of the crystallite sizes after 1, 2, 3 min and 2 h were 2.1, 1.6, 1.3, 1.02. According to our model, a value of 1.02 corresponds to a σ of 1.86 for a log-normal distribution. For n values higher than 1.3, our empirical relation no longer holds and we can only conclude that σ in such cases is larger than 2. The fast decrease of n in

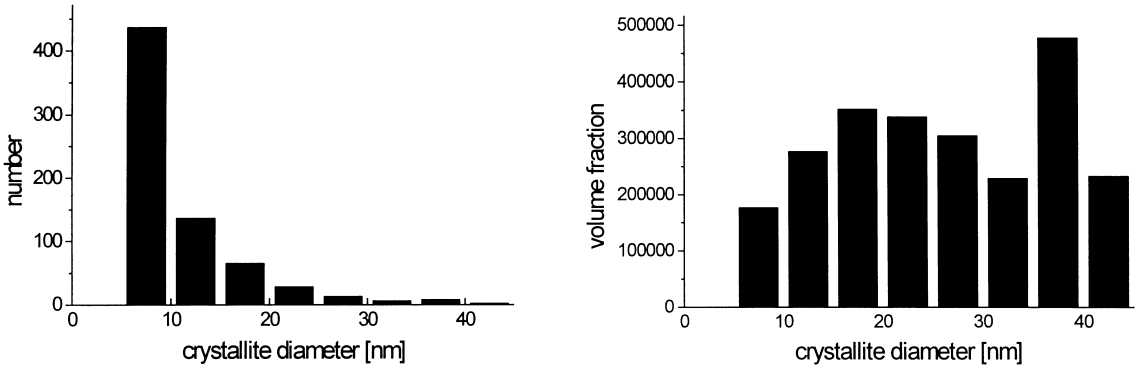

Fig. 5. Histograms to TEM-image in Fig. 4.

the first minutes shows that the smaller crystallites grow very quickly while the bigger ones hardly grow: the corresponding D_V values are 18, 21, 24, 32 nm.

5. Conclusion

Combustion synthesis is a simple, fast and cheap method to prepare nanocrystalline $SrTiO_3$ with a minimal apparative equipment. The properties of the ignition products depend strongly on the educt mixture composition and the ignition temperatures, and the choice of the right parameters makes it possible to obtain X-ray pure $SrTiO_3$. As will be discussed in part II of this paper, the ignition products with their different amounts and kinds of impurities exhibit remarkable differences in sintering behaviour.

Acknowledgements

This work was supported by the DFG in the frame of the Graduiertenkolleg 'Fundamental principles and technology of new high performance materials' and of SFB 277 'Interface determined materials'.

References

1. Shlom, D. G., Marshall, A. F., Sizemore, Z. J., Chen, J. N., Bozovic, I., von Dessonneck, K. E., Harris, J. S. and Bravman Jr., J. C., Molecular beam epitaxial growth of layered Bi–Sr–Ca–Cu–O-compounds. *J. Cryst. Growth*, 1990, **102**, 361–375.
2. Terashima, T., Bando, Y., Iijima, K., Yamamoto, K., Hirata, K., Kamigaki, K. and Terauchi, H., Reflection high-energy electron diffraction oscillations during epitaxial growth of high-temperature superconducting oxides. *Phys. Rev. Lett.*, 1990, **65**, 2684–2687.
3. Kawai, M., Watanabe, S. and Hanada, T., Molecular beam epitaxy of $Bi_2Sr_2CuO_x$ and $Bi_2Sr_2Ca_{0.85}Sr_{0.15}Cu_2O_x$ ultra thin films at 300°C. *J. Cryst. Growth*, 1991, **112**, 745–752.
4. Yeh, Y. C. and Tseng, T. Y., Humidity-sensitive properties of $Ba_{0.5}Sr_{0.5}TiO_3$ porous ceramics. *J. Mat. Sci. Lett.*, 1988, **7**, 766–768.
5. Chambonnot, D., Andry, C., Fages-Bonnery, A., Mer, C., Fages, C. and Perriere, J., Growth of BST thin films on silicon substrate, Applications to integrated capacitors for DC–DC converters. *J. Phys. France*, 1998, **8**(9), 213–216.
6. Dedyk, A. I., Karmanenko, S. F., Leppavuori, S. and Sakharov, V. I., Influence of layer interface parameters on dielectric characteristics of BSTO ferroelectric film planar capacitors. *J. Phys. France*, 1998, **8**(9), 217–220.
7. Hoffmann, S. and Waser, R., Curie–Weiss-law of $Ba_{1-x}Sr_xTiO_3$ thin films prepared by chemical solution deposition. *J. Phys. France*, 1998, **8**(9), 221–224.
8. Phule, P. P. and Risbud, S. H., Low-temperature synthesis and processing of electronic materials in the $BaO–TiO_2$-system. *J. Mat. Sci.*, 1990, **25**, 1169–1183.
9. Sekar, M. A., Dhanaraj, G., Phat, H. L. and Patil, K. C., Synthesis of fine-particle titanates by the pyrolysis of oxalate precursors. *J. Mat. Sci.; Mat. Electr.*, 1992, **3**, 237–239.
10. Leoni, M., Viviani, M., Nanni, P. and Buscaglia, V., Low-temperature aqueous synthesis (LTAS) of ceramic powders with perowskite structure. *J. Mat. Sci. Lett.*, 1996, **15**, 1302–1304.
11. Chien, A. T., Speck, J. S., Lange, F. F., Daykin, A. C. and Levi, C. G., Low temperature/low pressure hydrothermal synthesis of barium titanate: powder and heteroepitaxial thin films. *J. Mat. Res.*, 1995, **10**(7), 1784–1789.
12. McHale, J. M., McIntyre, P. C., Sickafus, K. E. and Coppa, N. V., Nanocrystalline $BaTiO_3$ from freeze-dried nitrate solutions. *J. Mat. Res.*, 1996, **11**(5), 1199–1209.
13. Zhong, Z. and Gallagher, P. K., Combustion synthesis and characterization of $BaTiO_3$. *J. Mat. Res.*, 1995, **10**(4), 945–952.
14. Sekar, M. A. and Patil, K. C., Combustion-synthesis of lead-based dielectrics: a comparative study of redox-compounds and mixtures. *Int. J. Self-Prop. High-Temp. Syn.*, 1994, **3**(1), 27–38.
15. Sekar, M. A. and Patil, K. C., Combustion-synthesis of fine-particle dielectric oxide materials. *J. Mat. Chem.*, 1992, **2**(7), 739–743.
16. Komarov, A. V. and Parkin, I. P., Self-propagating high-temperature synthesis of $BaTiO_3$ using titanium trichloride as a fuel source. *J. Mat. Sci. Lett.*, 1996, **15**, 542–543.
17. Haberkorn, R., *FormFit — A program for X-ray Powder Pattern Deconvolution and Determination of Microstructure*. Dudweiler, 1998.
18. Poth, J., Haberkorn, R. and Beck, H. P., Combustion synthesis of $SrTiO_3$ Part II. Sintering behaviour and surface characterisation. *J. Eur. Ceram. Soc.*, 2000, **20**.